ORGANOMETALLICS

Article

pubs.acs.org/Organometallics

Synthesis and Catalytic Evaluation of Ruthenium−Arene Complexes Bearing Imidazol(in)ium-2-thiocarboxylate Ligands

Morgan Hans,[†] Quentin Willem,[†] Johan Wouters,[‡] Albert Demonceau,[†] and Lionel Delaude*[,†]

[†]Laboratory of Macromolecular Chemistry and Organic Catalysis, Institut de Chimie (B6a), Université de Liège, Sart-Tilman par 4000 Liège, Belgium

[‡]Department of Chemistry, Facultés Universitaires N.-D. de la Paix, 61 Rue de Bruxelles, 5000 Namur, Belgium

Supporting Information

ABSTRACT: Five new complexes with the generic formula [$RuCl_2$(*p*-cymene)(SOC·NHC)] (**2**−**6**) were isolated in high yields by reacting the [$RuCl_2$(*p*-cymene)]$_2$ dimer with a range of imidazol(in)ium-2-thiocarboxylate zwitterions bearing cyclohexyl, 2,4,6-trimethylphenyl (mesityl), or 2,6-diisopropylphenyl groups on their nitrogen atoms in CH_2Cl_2 at −20 °C. All the products were fully characterized by IR and NMR spectroscopy, and the molecular structures of [$RuCl_2$(*p*-cymene)(SOC·IMes)] (**3**) and [$RuCl_2$(*p*-cymene)(SOC·SIMes)] (**5**) were determined by X-ray diffraction analysis. Coordination of the NHC·COS ligands took place via the sulfur atom. A remarkable shielding of the methine proton on the *p*-cymene isopropyl group was observed by ^{1}H NMR spectroscopy for complexes **3**−**6**. It is most likely caused by the aromatic ring current of a neighboring mesityl or 2,6-diisopropylphenyl substituent. The catalytic activity of compounds **2**−**6** was probed in the ring-opening metathesis polymerization (ROMP) of cyclooctene, in the atom transfer radical polymerization (ATRP) of methyl methacrylate, and in the synthesis of enol esters from 1-hexyne and 4-acetoxybenzoic acid. In all these reactions, the [$RuCl_2$(*p*-cymene)(SOC·NHC)] complexes displayed performances slightly inferior to those exhibited by [$RuCl_2$(*p*-cymene)(NHC)] species that result from the reaction of [$RuCl_2$(*p*-cymene)]$_2$ with NHC·CO_2 inner salts. However, they were significantly better catalyst precursors than the much more robust chelates of the [RuCl(*p*-cymene)(S_2C·NHC)]PF_6 type obtained by coordination of NHC·CS_2 betaines to the ruthenium dimer. These results suggest that the Ru−(SOC·NHC) motif undergoes a dethiocarboxylation under the experimental conditions adopted for the catalytic tests and leads to the same elusive Ru−NHC active species as the preformed [$RuCl_2$(*p*-cymene)(NHC)] family of complexes.

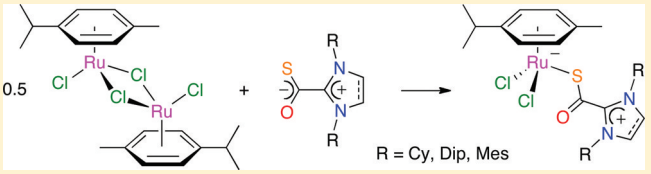

INTRODUCTION

Since they were first isolated by Arduengo in 1991,[1] stable N-heterocyclic carbenes (NHCs) based on the imidazole ring system have found countless applications in organocatalysis and organometallic chemistry.[2] Due to their high nucleophilicity, they readily add to a wide range of organic compounds, including allenes, ketenes, and heteroallenes of the X═C═Y type.[3] Upon reaction with carbon dioxide, they form inner salts, which can be stored and handled with no particular precautions.[4] Such NHC·CO_2 zwitterions readily lose their CO_2 moiety upon heating or dissolution. Hence, they act as convenient surrogates to air- and moisture-sensitive free carbenes for organometallic synthesis[5] and organocatalytic applications.[6] In 2006, we first took advantage of their lability to generate active species in palladium-catalyzed Suzuki−Miyaura cross-coupling reactions[7] and ruthenium-promoted olefin metathesis and cyclopropanation processes.[8] The next year, Beller and co-workers adopted a similar strategy to generate palladium−NHC catalysts in situ for the telomerization of 1,3-butadiene with amines.[9] In 2009, we further investigated the reactivity of imidazolium-2-carboxylates toward the [$RuCl_2$(*p*-cymene)]$_2$ dimer and we confirmed that these betaines cleanly underwent a decarboxylative cleavage upon heating to afford the corresponding [$RuCl_2$(*p*-cymene)(NHC)] complexes in high yields (Scheme 1).[10] This methodology was successfully

Scheme 1. Synthesis of Ruthenium−Arene Complexes Bearing NHC Ligands from [$RuCl_2$(*p*-cymene)]$_2$ and Imidazolium-2-carboxylates

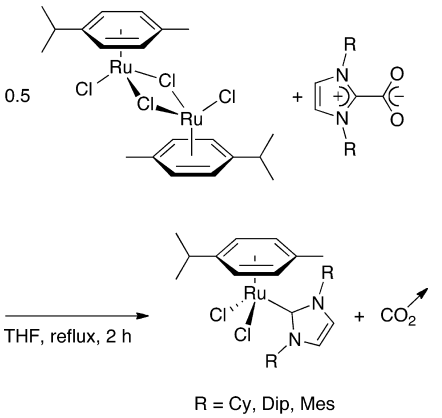

Received: July 20, 2011
Published: October 26, 2011

extended to the preparation of various second-generation ruthenium−alkylidene catalysts for olefin metathesis.[11,12]

Zwitterionic products are also obtained when carbon disulfide is reacted with NHCs or precursors thereof.[13] The NHC·CS_2 betaines differ from the NHC·CO_2 series in that the dithiocarboxylate moiety shows no significant lability upon reaction with metals.[3] The coordination chemistry of these stable crystalline compounds remained almost unexplored until 2009, when a report based on ruthenium−arene complexes provided strong experimental evidence for the formation of cationic species of the [RuCl(*p*-cymene)(S_2C·NHC)]$^+$ type, in which the dithiocarboxylate group acted as a κ^2S,S′ chelating ligand (Scheme 2).[10] Further investigations on ruthenium or

Scheme 2. Synthesis of Ruthenium−Arene Complexes Bearing Imidazol(in)ium-2-dithiocarboxylate Ligands

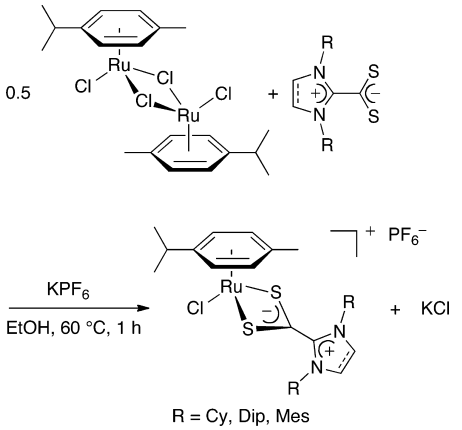

osmium−alkenyl compounds confirmed this binding mode, although the most bulky imidazolium-2-dithiocarboxylates under scrutiny displayed a noninnocent behavior in some instances, thereby allowing an unexpected migration of the alkenyl fragment to take place.[14] In 2010, the inorganic chemistry of NHC·CS_2 zwitterions was extended to the synthesis of gold(I) complexes and gold nanoparticles.[15] On the catalysis front, the activity of five [RuCl(*p*-cymene)-(S_2C·NHC)]PF_6 complexes was probed in various ring-closing metathesis (RCM) and ring-opening metathesis polymerization (ROMP) reactions but, as expected, these robust, 18-electron species were almost inactive.[10] Likewise, they were poorly active and selective catalyst precursors for the addition of 4-acetoxybenzoic acid to 1-hexyne. Their efficiency in the synthesis of enol esters markedly increased, however, when reactions were carried out at 160 °C under microwave or conventional heating in a sealed tube.[16]

In view of the rich chemistry exhibited by NHC·CO_2 and NHC·CS_2 betaines and the marked differences existing between these two types of compounds, we launched a program to investigate the structural properties and the reactivity of the related NHC·COS zwitterions. In our first article, we reported on the synthesis and characterization of five imidazol(in)ium-2-thiocarboxylates bearing alkyl or aryl groups on their nitrogen atoms and their use as organocatalysts for acylation/transesterification reactions and for the benzoin condensation.[17] Another publication focused on the use of these oxygen−sulfur mixed-donor ligands for the preparation of cationic gold(I) complexes.[18] In this contribution, we further investigate the coordination chemistry of NHC·COS betaines toward the [$RuCl_2$(*p*-cymene)]$_2$ dimer. More specifically, we describe the synthesis of five ruthenium−arene complexes based on these zwitterionic ligands and we probe their ability to serve as catalyst precursors for olefin metathesis, atom transfer radical polymerization, and enol ester synthesis.

RESULTS AND DISCUSSION

Synthesis of Ruthenium−Arene Complexes. In order to prepare [$RuCl_2$(*p*-cymene)(NHC)] complexes, the [$RuCl_2$(*p*-cymene)]$_2$ dimer was refluxed for 2 h in THF with 2 equiv of NHC·CO_2 zwitterions (cf. Scheme 1). In these experiments, a slow stream of argon was applied on top of the condenser to help displace carbon dioxide.[10] When NHC·CS_2 betaines were reacted under the same conditions, elimination of carbon disulfide did not occur, even after prolonged heating. The coordination of these stable inner salts to a ruthenium center was accomplished by heating stoichiometric amounts of [$RuCl_2$(*p*-cymene)]$_2$ (1 equiv), an imidazol(in)ium-2-dithiocarboxylate, and KPF_6 (2 equiv each) for 1 h at 60 °C in ethanol (cf. Scheme 2). This simple aerobic protocol afforded a series of complexes with the generic formula [RuCl(*p*-cymene)(S_2C·NHC)]PF_6 in high yields and purities.[10] Because thermogravimetric analyses had shown that NHC·COS betaines displayed a thermal stability intermediate between those of NHC·CO_2 and NHC·CS_2 adducts,[17] we decided to probe their reactivity toward the ruthenium dimer using both experimental procedures. Zwitterions derived from five representative saturated or unsaturated NHCs bearing mesityl (Mes), 2,6-diisopropylphenyl (Dip), or cyclohexyl (Cy) substituents on their nitrogen atoms were elected as starting materials for these investigations (Scheme 3). Unfortunately, all

Scheme 3. Imidazol(in)ium-2-thiocarboxylates Used in This Work

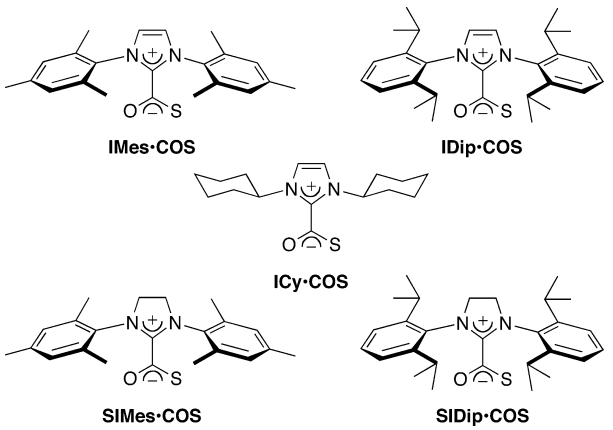

our attempts to isolate pure compounds resulting from a full dethiocarboxylation or chelation of these imidazol(in)ium-2-thiocarboxylates failed. In all these exploratory trials, complex mixtures of unidentified products were always obtained. Among other things, we noted that decreasing the temperature usually led to cleaner reaction mixtures and that KPF_6 did not seem to have any influence on the reaction course. Replacement of this salt with $AgBF_4$ to ease the abstraction of a chloro ligand and the formation of a cationic κ^2O,S chelate was equally ineffective.

On the basis of the observations described above, we devised a new strategy to favor the coordination of the thiocarboxylate group onto ruthenium as a monodentate ligand. To achieve this

dx.doi.org/10.1021/om2006529|*Organometallics* 2011, 30, 6133−6142

goal, reactions were performed in dichloromethane at low temperature under a static inert atmosphere. Initial experiments were carried out at room temperature or at 0 °C. Subsequently, we found that the best results were obtained when $[RuCl_2(p\text{-cymene})]_2$ (**1**) and a NHC·COS adduct in 1:2 molar proportions were stirred for 1 h in an ice/salt bath maintained at −20 °C (Scheme 4). Under these conditions, five new

Scheme 4. Synthesis of Ruthenium−Arene Complexes Bearing Imidazol(in)ium-2-thiocarboxylate Ligands

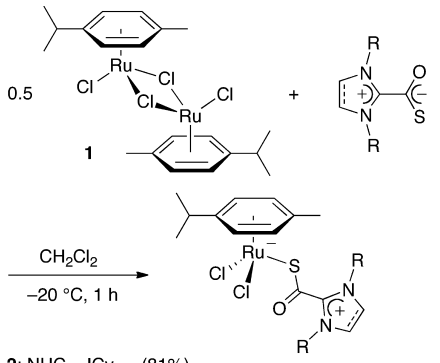

ruthenium−arene complexes with the generic formula $[RuCl_2(p\text{-cymene})(SOC{\cdot}NHC)]$ were isolated in high yields after a simple workup that involved solvent removal and washing with *n*-pentane. Compounds **2**−**6** were obtained as orange microcrystalline powders and fully characterized by various analytical techniques. Except for the SIMes derivative (**5**), they were all very soluble in CH_2Cl_2 and $CHCl_3$. Their stability in solution was, however, limited, especially in the presence of air and moisture. ^{1}H NMR monitoring of a CD_2Cl_2 solution of complex **3** in a capped tube under an inert atmosphere showed that it reverted to $[RuCl_2(p\text{-cymene})]_2$ (**1**) and IMes·COS within a few hours at 40 °C. Adding a stoichiometric amount of triphenylphosphine to complex **5** in CD_2Cl_2 at room temperature led to the instantaneous formation of $[RuCl_2(p\text{-cymene})(PPh_3)]$, as evidenced by ^{1}H and ^{31}P NMR analyses. In the solid state, compounds **2**−**6** could be kept in open-air vials for more than 6 months at room temperature without showing any sign of decomposition on ^{1}H NMR spectroscopy.

Structural Analysis. In order to minimize degradation during the period of time required for ^{13}C acquisition, NMR spectra of complexes **2**−**6** were recorded in CD_2Cl_2 at 263 or 273 K. Most resonances fell within the usual ranges of chemical shifts expected for coordinated arene[19] and imidazol(in)ium-2-thiocarboxylate ligands.[18] For instance, ^{1}H NMR analysis showed the presence of two doublets located between 5.1 and 5.7 ppm with a common coupling constant of ca. 6 Hz for the aromatic protons of the η^6-(*p*-cymene) ligand, while ^{13}C NMR spectra displayed a strongly deshielded signal at ca. 186 ppm, due to the COS group. A puzzling anomaly was, however, detected for the methine protons of the *p*-cymene isopropyl group in complexes **3**−**6**. Indeed, the characteristic septet of the $ArCH(CH_3)_2$ motif was located between 1.6 and 1.9 ppm in these compounds, more than 1 ppm upfield from its usual position recorded at 2.83 ppm in $[RuCl_2(p\text{-cymene})(SOC{\cdot}ICy)]$ (**2**). HMBC and HSQC experiments confirmed these assignments. We attribute this large discrepancy to a remarkable shielding effect, due to a favorable spatial disposition between the methine proton and the aromatic ring of a neighboring mesityl or 2,6-diisopropylphenyl group (vide infra).

In addition to the various C−C and C−H vibration bands, three major absorptions were clearly visible in the FT-IR spectra of the five ruthenium−arene complexes under investigation (Table 1). They were assigned to the stretching

Table 1. IR Stretching Vibration Bands of $[RuCl(p\text{-cymene})(SOC{\cdot}NHC)]$ Complexes (2−6) and NHC·COS Zwitterions[a]

	$[RuCl_2(p\text{-cymene})(SOC{\cdot}NHC)]$			NHC·COS		
NHC	$\bar{\nu}_{CO}$ (cm^{-1})	$\bar{\nu}_{CN}$ (cm^{-1})	$\bar{\nu}_{CS}$ (cm^{-1})	$\bar{\nu}_{CO}$ (cm^{-1})[b]	$\bar{\nu}_{CN}$ (cm^{-1})[b]	$\bar{\nu}_{CS}$ (cm^{-1})[b]
ICy	1571	1482, 1451	934	1524	1484, 1450	954
IMes	1568	1488, 1469	910	1532	1486, 1464	917
IDip	1572	1474	917	1531	1479	937
SIMes	1558	1482, 1470	1029	1545	1483	1050, 1037
SIDip	1573, 1553	1465, 1444	1043	1559, 1538	1465, 1445	1045

[a]Spectra were recorded in KBR pellets. [b]Data from ref 17.

of the CO, CN, and CS bonds within the imidazol(in)ium-2-thiocarboxylate ligands by comparison with values previously reported for miscellaneous imidazol(in)ium[20] or thiocarboxylate derivatives.[21,22] In some instances, these absorptions were further split into two components, both of which are given in Table 1. It should be pointed out that all these assignments are tentative and should be taken with caution. For the sake of comparison, the corresponding $\bar{\nu}_{CO}$, $\bar{\nu}_{CN}$, and $\bar{\nu}_{CS}$ values recorded for the free NHC·COS zwitterions are also included in Table 1.[17] The $\bar{\nu}_{CN}$ wavenumbers did not vary significantly upon binding to the ruthenium center, which indicates that the imidazol(in)ium moieties of the ligands were not affected by complexation. These results are in line with the general observation that there is no electronic communication between the anionic and the cationic parts of NHC·CXY adducts (X, Y = O, S, Se).[10,23] Conversely, the formation of complexes **2**−**6** markedly influenced the IR signatures of the thiocarboxylate group. The CS stretching band was systematically shifted to *lower* frequencies upon coordination, whereas the CO absorption occurred at *higher* energies. These variations strongly suggest that coordination of the COS^- unit to the metal center takes place via its sulfur atom only, thereby weakening the CS bond and strengthening the CO bond.[21]

To establish with certainty that NHC·COS zwitterions acted as monodentate S-ligands in ruthenium−arene complexes, we determined the molecular structures of compounds **3** and **5** by X-ray diffraction analysis. Crystals of $[RuCl_2(p\text{-cymene})(SOC{\cdot}SIMes)]$ (**5**) were obtained from a concentrated solution in dichloromethane cooled to −18 °C. In the case of $[RuCl_2(p\text{-cymene})(SOC{\cdot}IMes)]$ (**3**), *n*-pentane was added to further decrease the polarity of the cold solution. Both solids crystallized in the monoclinic system and belonged to the same $P2_1/c$ group. Thus, replacement of the 1,3-dimesitylimidazolium ring in product **3** with its saturated imidazolinium counterpart in **5** had only a very limited impact on the crystal structure. Because the molecular parameters of free SIMes·COS

dx.doi.org/10.1021/om2006529|*Organometallics* 2011, 30, 6133−6142

are available for comparison,[17] only data pertaining to complex **5** are discussed here (see the Supporting Information for more details on the crystal structure of complex **3** and an ORTEP plot).

As anticipated, the metal center in [$RuCl_2$(*p*-cymene)(SOC·SIMes)] (**5**) displayed the distinctive three-legged piano-stool geometry observed in many other ruthenium–arene species[24] and was connected to the zwitterionic ligand via its sulfur atom (Figure 1). Bond lengths and angles determined

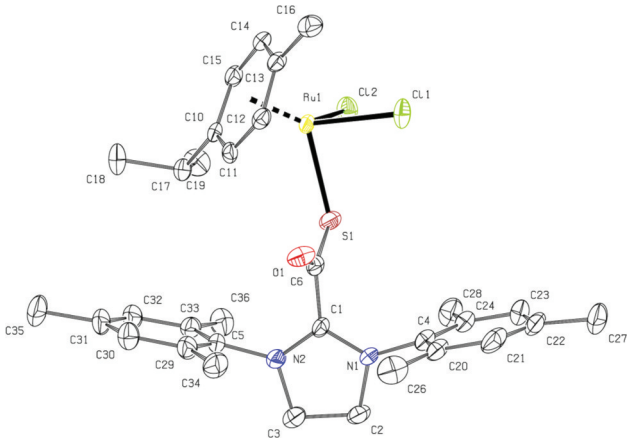

Figure 1. ORTEP representation of [$RuCl_2$(*p*-cymene)(SOC·SIMes)] (**5**) with thermal ellipsoids drawn at the 50% probability level (hydrogen atoms are omitted for the sake of clarity). Selected bond lengths (Å) and angles (deg): C1–C6 = 1.517(9), C6–O1 = 1.227(13), C6–S1 = 1.688(8), C1–N1 = 1.317(12), C1–N2 = 1.306(11), C2–C3 = 1.522(13), N1–C4 = 1.442(11), N2–C5 = 1.449(12), Ru1–Cl1 = 2.412(2), Ru1–Cl2 = 2.408(3), Ru1–S1 = 2.391(3); N1–C1–N2 = 113.2(8), O1–C6–S1 = 131.9(7); N1–C1–C6–S1 = 80.4(1), C1–N1–C4–C20 = 82.2(1), C1–N2–C5–C29 = −84.5(4).

previously for the free SIMes·COS adduct[17] remained largely unaffected by coordination, except for the torsion angle between the imidazolinium ring and the thiocarboxylate unit, which was reduced from 95.0(1) to 80.4(1)°, probably due to steric reasons. At 1.227(13) Å, the C–O distance was much closer to values commonly reported for C=O double bonds (1.210(8) Å) than for single bonds (1.423(18) Å).[25] The C–S bond length of 1.682(8) Å in complex **5** is also indicative of electron delocalization within the COS moiety, as this bond is much closer to the values reported for C=S double bonds (1.671(24) Å) than for single C–S bonds (1.808(10) Å). Last but not least, the Ru–S bond length of 2.3897(17) Å was similar to those recorded previously in related monodentate ruthenium–thiocarboxylate complexes,[21,22] whereas the much greater distance between the metal center and the terminal oxygen (3.64 Å) precluded any interaction between these two atoms.

A careful inspection of the molecular structures of complexes **3** and **5** revealed that, in the solid state, the methine proton of the *p*-cymene isopropyl group was pointing toward the center of the neighboring mesityl ring. Indeed, trigonometric calculations showed that H17 was located 3.132 Å from the centroid defined by C5 and C29–C33, with a deviation to orthogonality of 28.670° for [$RuCl_2$(*p*-cymene)(SOC·IMes)] (**3**) (Figure 2). Similar values of H17–Cg (3.151 Å) and H17_perp (31.068°) were obtained from the crystal structure of [$RuCl_2$(*p*-cymene)(SOC·SIMes)] (**5**). We believe that this geometry is responsible for the unusually low chemical shift recorded for H17 in complexes **3**–**6** in ^{1}H NMR spectroscopy (vide supra). Indeed, hydrogen nuclei located over an aromatic ring are known to experience a substantial shielding caused by the magnetic field induced by the π-electron circulation.[26] This anisotropic effect is reminiscent of the significant high-field shift observed for one of the aromatic mesityl protons in *cis*-dichlororuthenium benzylidene complexes under the influence of π–π stacking.[27] In the related complex [RuCl(*p*-cymene)-(S_2C·IMes)]PF_6 (**7**),[10] which has an intermediate chelating CS_2^- group between the carbenoid ligand and the metal center, and [$RuCl_2$(*p*-cymene)(IMes)] (**8**)[28] sporting a direct Ru–NHC bond, the corresponding methine proton was located much farther away from the neighboring mesityl ring, thereby precluding any magnetic interaction (Figure 2).

Catalytic Tests. In order to assess the catalytic efficiency of complexes **2**–**6**, we first investigated the ROMP of cyclooctene in chlorobenzene at 60 °C for 2 h using a monomer-to-catalyst ratio of 250 (Scheme 5). In our laboratory, the polymerization

Scheme 5. ROMP of Cyclooctene

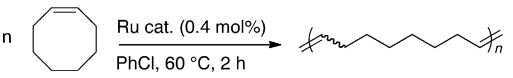

of this low-strain cycloolefin is commonly used as a benchmark to evaluate the metathetical activity of new ruthenium–arene complexes.[12,29] An ordinary neon tube placed 10 cm away from

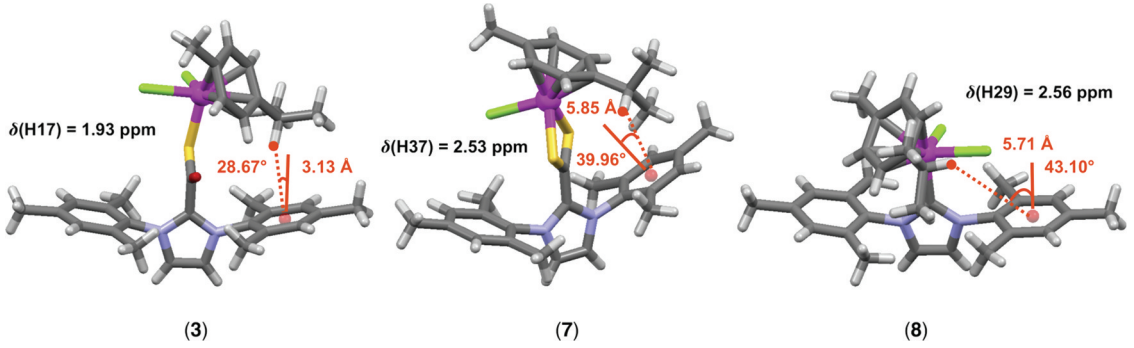

Figure 2. Molecular structures of [$RuCl_2$(*p*-cymene)(SOC·IMes)] (**3**), [RuCl(*p*-cymene)(S_2C·IMes)]PF_6 (**7**), and [$RuCl_2$(*p*-cymene)(IMes)] (**8**), showing the orientation of the methine proton on the *p*-cymene isopropyl group relative to the neighboring mesityl ring and its ^{1}H NMR chemical shift.

dx.doi.org/10.1021/om2006529|*Organometallics* 2011, 30, 6133–6142

the Pyrex reaction flasks ensured a strong, reproducible lighting. Previous investigations had shown that visible light was required to generate metathetically active species from [$RuCl_2$(*p*-cymene)(NHC)] precursors, most likely via a total or partial decoordination of the η^6-arene ligand.[30,31] Despite such a photochemical activation,[32] conversion of cyclooctene stagnated below 25% with all the [$RuCl_2$(*p*-cymene)-(SOC•NHC)] complexes under study (Table 2). White fibers

Table 2. ROMP of Cyclooctene Catalyzed by Various Ruthenium−Arene Complexes[a]

cat.	monomer conversn (%)[b]	polymer yield (%)	M_n(kg mol^{-1})[c]	M_w/M_n[c]	σ_{cis}[d]
2	21	traces			
3	18	9	713	2.1	0.39
4	17	5	0.3	2.6	0.35
5	19	15	727	1.8	0.35
6	18	traces			
7	1				
8	95	85	715	2.0	0.25

[a]Experimental conditions: Ru cat. (0.03 mmol), cyclooctene (1 mL, 7.5 mmol), PhCl (5 mL), 2 h at 60 °C under visible light illumination. [b]Determined by GC using cyclooctane as internal standard. [c]Determined by SEC in THF with polystyrene calibration. [d]Fraction of cis double bonds in the polymer, determined by ^{13}C NMR spectroscopy.

of high-molecular-weight polyoctenamer containing mostly trans double bonds were isolated with catalyst precursors **3** and **5** containing respectively the IMes•COS and SIMes•COS ligands, while [$RuCl_2$(*p*-cymene)(SOC•IDip)] (**4**) afforded a small amount of ruthenium-tainted macromolecular product with a low molecular weight and a broad polydispersity. In the case of complexes **2** and **6**, only traces of polymer precipitated from the reaction mixtures. Soluble, uncharacterized oligomers probably accounted for the mass balance.

For the sake of comparison, we also carried out the ROMP of cyclooctene with [RuCl(*p*-cymene)(S_2C•IMes)]PF_6 (**7**), as a representative complex bearing a NHC•CS_2 ligand, and [$RuCl_2$(*p*-cymene)(IMes)] (**8**), which results from the reaction of [$RuCl_2$(*p*-cymene)]$_2$ (**1**) with IMes•CO_2 (Table 2). In line with previous observations,[10] the former cationic chelate was completely inefficient, whereas the latter well-known initiator afforded an almost quantitative conversion of monomer into a high-molecular-weight polymer. It is worth emphasizing that complex **3**, based on the 1,3-dimesitylimidazolium-2-thiocarboxylate ligand, ranked between these two extremes. Furthermore, when examining the influence of the NHC moiety on the activity of complexes **2**−**6**, we observed the same trends as those recorded for preformed [$RuCl_2$(*p*-cymene)-(NHC)] complexes or, alternatively, for active species generated in situ from [$RuCl_2$(*p*-cymene)]$_2$ (**1**), an imidazol(in)ium salt, and a base. Indeed, structure−activity relationships derived from these catalytic systems had shown that (i) NHCs with N-aryl substituents performed much better than those with N-alkyl groups such as ICy, (ii) the C=C double bond in the imidazole ring of the NHC was not crucial to achieve high catalytic efficiencies, and (iii) the IMes and SIMes ligands proved superior to the more bulky IDip and SIDip for polymerizing cyclooctene.[30,33] Hence, we suspect that [$RuCl_2$(*p*-cymene)-(SOC•NHC)] complexes are converted into the same elusive Ru−NHC active species as their [$RuCl_2$(*p*-cymene)(NHC)] counterparts under the experimental conditions adopted for ROMP, although with a much reduced efficiency. This hypothesis is supported by the fact that complexes **2**−**6** are labile in solution and that NHC•COS zwitterions are liable to release free carbenes upon thermolysis.[17] To gain further evidence in favor of this assumption, we refluxed a solution of complex **3** in THF for 2 h under a slow stream of argon. NMR analysis of the residue isolated after solvent evaporation and purification through a short plug of alumina showed the presence of [$RuCl_2$(*p*-cymene)(IMes)] (**8**), but other unidentified byproducts were also present in larger proportions.

Next, we focused our attention on the ruthenium-promoted atom transfer radical polymerization (ATRP) of methyl methacrylate (MMA) initiated by ethyl 2-bromo-2-methylpropanoate (Scheme 6). The monomer and the initiator were

Scheme 6. ATRP of MMA

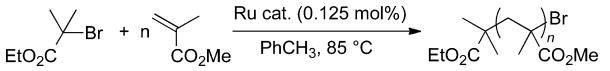

stirred in an oil bath at 85 °C in the presence of complexes **2**−**6** until a highly viscous solution was obtained and the magnetic stirring bar was immobilized. The initial monomer/initiator/ruthenium molar proportions were 800:2:1. Under these conditions, complexes **4** and **6** bearing 2,6-diisopropylphenyl-substituted ligands did not afford a controlled polymerization. Instead, they led to high-molecular-weight PMMA with a rather broad polydispersity, thereby causing a rapid gelation of the reaction mixtures (Table 3). Catalyst precursors **3** and **5**

Table 3. ATRP of MMA Catalyzed by Various Ruthenium−Arene Complexes[a]

cat.	reacn time (h)	polymer yield (%)	M_n (kg mol^{-1})[b]	M_w/M_n[b]
2	48	80	97	1.56
3	100	59	41	1.59
4	10	49	208	1.62
5	100	59	68	1.59
6	16	50	224	1.63
7	100	42	52	1.68
8[c]	16	49	28	1.35

[a]Experimental conditions: Ru cat. (0.0117 mmol), 0.1 M ethyl 2-bromo-2-methylpropanoate in toluene (0.25 mL, 0.025 mmol), MMA (1 mL, 9.35 mmol), 85 °C. [b]Determined by SEC in THF with PMMA calibration. [c]Data from ref 34.

bearing respectively the IMes•COS and SIMes•COS ligands displayed a higher initiation efficiency and gave polymers whose molecular weights matched more closely those expected for a well-behaved system (40 kg mol^{-1}). At 1.59, the polydispersity index obtained with these two complexes denoted, however, that control was not optimal. With [$RuCl_2$(*p*-cymene)-(SOC•ICy)] (**2**) a slightly narrower molecular weight distribution and a better yield were obtained, but the molecular weight exceeded the target value by far.

Control experiments carried out with [RuCl(*p*-cymene)-(S_2C•IMes)]PF_6 (**7**) and [$RuCl_2$(*p*-cymene)(IMes)] (**8**) helped us to better assess the influence of imidazol(in)ium-2-thiocarboxylate ligands on the catalytic activity of ruthenium−arene complexes (Table 3). As was observed for the ROMP of cyclooctene, complex **3** was a much better catalyst precursor for the ATRP of MMA than the corresponding dithiocarboxylate

dx.doi.org/10.1021/om2006529|*Organometallics* 2011, 30, 6133−6142

Scheme 7. Synthesis of Enol Esters from 4-Acetoxybenzoic Acid and 1-Hexyne

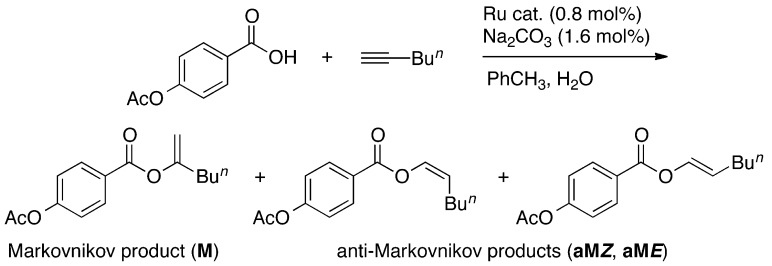

chelate (**7**), but displayed inferior performances compared to the imidazolylidene-based complex **8**.

To further appraise the potentials of complexes **2**–**6** in homogeneous catalysis, we probed their activity in the synthesis of enol esters. Indeed, various types of ruthenium–arene complexes are known to catalyze the addition of carboxylic acids to terminal alkynes, thereby affording vinyl esters in high yields and with excellent selectivities.[35] The hydrooxycarbonylation of 1-hexyne with 4-acetoxybenzoic acid was chosen as a model reaction for these investigations (Scheme 7). Experimental protocols that proved successful for enhancing the catalytic activity of [RuCl(*p*-cymene)(S_2C·NHC)]PF_6 and [$RuCl_2$(*p*-cymene)(NHC)] complexes in earlier studies were employed again.[16] Thus, water-saturated toluene was used as a solvent and sodium carbonate was added as an activator.[36] Separation and quantification of the three possible products, viz., 1-hexen-2-yl 4-acetoxybenzoate (Markovnikov addition product, **M**) and the *E* and *Z* isomers of 1-hexen-1-yl 4-acetoxybenzoate (anti-Markovnikov addition products, **aM*E*** and **aM*Z***) were achieved by gas chromatography in the presence of *n*-dodecane as an internal standard. Because 1-hexyne was introduced in excess compared to the carboxylic acid (1.5 equiv), dimerization products of this terminal alkyne were also detected in the reaction media. In all cases, however, they represented less than 1% of the total conversion.

In a first series of experiments, we performed a rapid catalytic screening of the five ruthenium–thiocarboxylate complexes at our disposal using pressure vials and a monomodal microwave reactor. As demonstrated in 2009, such a device was very convenient to quickly heat the reaction mixtures at temperatures well above the boiling point of 1-hexyne (71–72 °C) and to speed up the synthesis of enol esters.[37] As a matter of fact, the microwave-assisted addition of 4-acetoxybenzoic acid to 1-hexyne catalyzed by complexes **2**–**5** afforded high yields of products after 10 min at 140 °C (Table 4). Only complex **6** stood below the 50% threshold under these conditions. In terms of selectivity, there was a marked dichotomy between complexes **2**–**4** prepared from imidazolium-2-thiocarboxylate zwitterions, which strongly favored the formation of the Markovnikov adduct (**M**), and complexes **5** and **6** bearing respectively the SIMes·COS and SIDip·COS ligands that afforded rather similar proportions of the three possible products. Furthermore, monitoring the evolution of the product distribution over a 30 min period under microwave irradiation at 140 °C showed that the selectivity significantly changed with time in the case of complexes **2**–**4**, whereas it remained almost invariant with catalyst precursor **6** and underwent only slight modifications with **5** (see the Supporting Information for kinetic plots).

Table 4. Microwave-Assisted Synthesis of Enol Esters Catalyzed by [$RuCl_2$(*p*-cymene)(SOC·NHC)] Complexes (2–6)[a]

		product distribution (%)[b]		
cat.	yield (%)[b]	**M**	**aMZ**	**aME**
2	84	68	23.5	8.5
3	84	77	19	4
4	67	58	34	8
5	61	35.5	35	29.5
6	35	18.5	43.5	38

[a]Experimental conditions: Ru cat. (0.004 mmol), Na_2CO_3 (0.008 mmol), 4-acetoxybenzoic acid (0.5 mmol), 1-hexyne (0.75 mmol), water-saturated toluene (2.6 mL), 10 min at 140 °C. [b]Determined by GC using *n*-dodecane as internal standard.

To better apprehend the influence of NHC·COS ligands on the outcome of the reaction, we performed a second series of more thorough catalytic tests on the addition of 4-acetoxybenzoic acid to 1-hexyne (Scheme 7). These experiments were carried out on a larger scale using Schlenk tubes placed in an oil bath at 60 °C. With this revised setup, the formation of enol esters was slowed down and it was possible to monitor more carefully and more conveniently the reaction course than in the microwave reactor. Time needed to reach completion was considerably longer, and differences between the various catalysts under investigation were more pronounced. Under these conditions, [$RuCl_2$(*p*-cymene)(SOC·ICy)] (**2**) emerged as the most efficient catalyst precursor among the five ruthenium–thiocarboxylate complexes under study (Table 5). Indeed, this compound afforded

Table 5. Synthesis of Enol Esters Catalyzed by Various Ruthenium–Arene Complexes[a]

		product distribution (%)[b]		
cat.	yield (%)[b]	**M**	**aMZ**	**aME**
2	100	83.5	13.5	3
3	66	79	16.5	4.5
4	44	71	20	9
5	23	20	36	44
6	21	20	38	42
9[c]	11	24	42	34
10[c]	99	83	14	3

[a]Experimental conditions: Ru cat. (0.0092 mmol), Na_2CO_3 (0.0184 mmol), 4-acetoxybenzoic acid (1.15 mmol), 1-hexyne (1.725 mmol), water-saturated toluene (6 mL), 50 h at 60 °C. [b]Determined by GC using *n*-dodecane as internal standard. [c]Data from ref 16.

dx.doi.org/10.1021/om2006529|*Organometallics* 2011, 30, 6133–6142

a quantitative reaction within 50 h, whereas its most serious contender, [$RuCl_2$(*p*-cymene)(SOC·IMes)] (**3**), led to a 66% yield within the same period of time. Altogether, the duration needed to reach completion followed the sequence **2** (50 h) < **3** (100 h) < **4** (150 h) ≪ **5** (535 h) < **6** (650 h) (see the Supporting Information for kinetic plots). Complex **2** was also the most selective catalyst precursor and strongly favored the formation of the Markovnikov adduct. However, it should be pointed out that the product distribution did not remain constant during the whole run. As noticed previously in the microwave-assisted reactions, the proportion of 1-hexen-2-yl 4-acetoxybenzoate (**M**) progressively increased over time to reach a final value of ca. 84% (Figure 3).

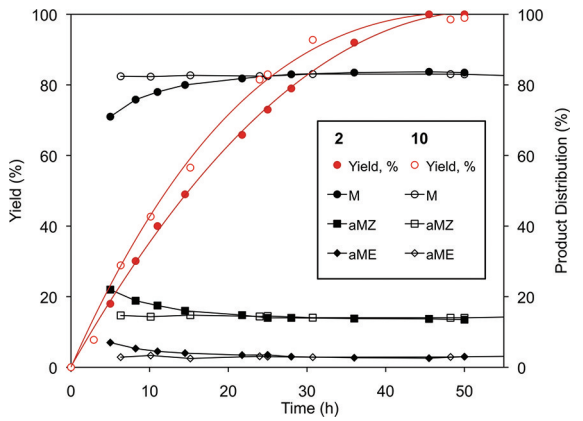

Figure 3. Time course of the addition of 4-acetoxybenzoic acid to 1-hexyne catalyzed by [$RuCl_2$(*p*-cymene)(SOC·ICy)] (**2**) and [$RuCl_2$(*p*-cymene)(ICy)] (**10**) in an oil bath at 60 °C.

Comparison of the results obtained with [$RuCl_2$(*p*-cymene)(SOC·ICy)] (**2**) and those reported previously for [RuCl(*p*-cymene)(S_2C·ICy)]PF_6 (**9**) and [$RuCl_2$(*p*-cymene)(ICy)] (**10**) showed that the Ru−thiocarboxylate and Ru−NHC complexes afforded almost identical yields and selectivities after 50 h (Table 5). Conversely, the dithiocarboxylate chelate was largely inefficient at promoting the hydrooxycarbonylation of 1-hexyne with 4-acetoxybenzoic acid at 60 °C and required microwave irradiation at 160 °C to become active.[16] A close examination of the reaction profiles of complexes **2** and **10** nevertheless revealed the existence of some minor, albeit significant, differences between these two catalyst precursors. In particular, monitoring the product distribution over time clearly showed that [$RuCl_2$(*p*-cymene)(ICy)] (**10**) led to invariant proportions of the three possible products from the early stage of the reaction to its completion, whereas the same final distribution was attained only after ca. 25 h, with complex **2** sporting an intermediate COS group between the metal center and the carbenoid moiety (Figure 3). Moreover, the reaction occurred slightly more quickly with complex **10** than with catalyst precursor **2**. The same trends were observed when comparing complexes **3** and **4** with the corresponding [$RuCl_2$(*p*-cymene)(NHC)] species (see the Supporting Information). These data suggest that complexes **2**−**4** containing an imidazolium-2-thiocarboxylate zwitterion might undergo a progressive dethiocarboxylation leading to active species bearing an imidazol-2-ylidene ligand under the experimental conditions adopted for enol ester synthesis. A similar transformation was already assumed to take place during the ROMP of cyclooctene at 60 °C (vide supra). The poor results obtained with precursors **5** and **6** in the present catalytic system further support the intermediacy of [$RuCl_2$(*p*-cymene)(NHC)] complexes —or active species derived thereof—because SIMes and SIDip are known to coordinate much more reluctantly to a ruthenium−arene scaffold than their aromatic counterparts IMes and IDip.[38]

In a third and final series of experiments, we examined the possibility of generating active species in situ from the [$RuCl_2$(*p*-cymene)]$_2$ dimer (**1**) and an imidazol(in)ium-2-(thio)carboxylate. The addition of 4-acetoxybenzoic acid to 1-hexyne was chosen once again as a case study for these catalytic tests (Scheme 7). Results gathered in Table 6 showed that a 1:2

Table 6. Synthesis of Enol Esters Catalyzed by Various Ruthenium−Arene Complexes Generated in Situ from [$RuCl_2$(*p*-cymene)]$_2$ (1) and 1,3-Dimesitylimidazol(in)ium Zwitterions[a]

		product distribution (%)[b]		
cat.	yield (%)[b]	**M**	**aMZ**	**aME**
1	26	18	37.5	44.5
1 + IMes·COS	48	77.5	17	5.5
1 + IMes·CO_2	48	76	17.5	6.5
1 + SIMes·COS	22	23	34.5	42.5

[a]Experimental conditions: [$RuCl_2$(*p*-cymene)]$_2$ (0.0046 mmol), NHC·CXY (0.0092 mmol), Na_2CO_3 (0.0184 mmol), 4-acetoxybenzoic acid (1.15 mmol), 1-hexyne (1.725 mmol), water-saturated toluene (6 mL), 50 h at 60 °C. [b]Determined by GC using *n*-dodecane as internal standard.

mixture of the ruthenium dimer and IMes·COS was less active than [$RuCl_2$(*p*-cymene)(SOC·IMes)] (**3**), as the yield dropped from 66% to 48% after 50 h at 60 °C (cf. Table 5). Accordingly, it took ca. 130 h to reach a complete conversion with the two-component mixture vs 100 h with the preformed complex (see the Supporting Information). Eventually, both systems afforded almost identical product distributions, suggesting that the same active species were at play. It is noteworthy that the replacement of 1,3-dimesitylimidazolium-2-thiocarboxylate with the corresponding carboxylate inner salt did not affect the reaction rate but led to the same differences in the evolution of selectivity that were already observed when comparing preformed [$RuCl_2$(*p*-cymene)(NHC)] and [$RuCl_2$(*p*-cymene)(SOC·NHC)] complexes (cf. Figure 3). Two supplementary trials were performed with [$RuCl_2$(*p*-cymene)]$_2$ (**1**) alone or in the presence of SIMes·COS (Table 6). Results from these control experiments unambiguously proved that the imidazolinium betaine did not have any significant influence on the reaction outcome, as the activity of the ruthenium−arene dimer (**1**) matched those displayed by [$RuCl_2$(*p*-cymene)(SOC·SIMes)] (**5**) either preformed or generated in situ. The same reaction profile had also been recorded with [$RuCl_2$(*p*-cymene)(SOC·SIDip)] (**6**) (cf. Table 5). These data confirm the crucial importance of choosing a NHC ligand based on the *imidazole* ring system rather than the *imidazoline* cycle to achieve high catalytic efficiencies in the synthesis of enol esters.

CONCLUSION

By reacting the [$RuCl_2$(*p*-cymene)]$_2$ dimer (**1**) with 2 equiv of NHC·COS betaines in dichloromethane at −20 °C, we were able to synthesize five new ruthenium−arene complexes bearing

dx.doi.org/10.1021/om2006529|*Organometallics* 2011, 30, 6133−6142

imidazol(in)ium-2-thiocarboxylate ligands coordinated to the metal center via their sulfur atom. Thus, complexes **2**–**6** with the generic formula [$RuCl_2$(*p*-cymene)(SOC·NHC)] were isolated in high yields and fully characterized by various analytical techniques. These compounds remained stable in the solid state for more than 6 months in the open air but were rather labile in solution. A remarkable shielding of the methine proton on the *p*-cymene isopropyl group was observed by ^{1}H NMR spectroscopy for complexes **3**–**6**. It is most likely caused by the aromatic ring current of a neighboring mesityl or 2,6-diisopropylphenyl substituent, as evidenced by a detailed analysis of the molecular structure of complexes **3** and **5**.

The catalytic activity of compounds **2**–**6** was probed in the ring-opening metathesis polymerization of cyclooctene, in the atom transfer radical polymerization of methyl methacrylate, and in the synthesis of enol esters from 1-hexyne and 4-acetoxybenzoic acid. In all these reactions, the [$RuCl_2$(*p*-cymene)(SOC·NHC)] complexes displayed performances slightly inferior to those exhibited by [$RuCl_2$(*p*-cymene)(NHC)] species that result from the reaction of [$RuCl_2$(*p*-cymene)]$_2$ with NHC·CO_2 inner salts. However, they were significantly better catalyst precursors than the much more robust chelates of the [RuCl(*p*-cymene)(S_2C·NHC)]PF_6 type obtained by coordination of NHC·CS_2 zwitterions to the ruthenium dimer. These results suggest that the Ru–(SOC·NHC) motif undergoes a dethiocarboxylation under the experimental conditions adopted for the catalytic tests and leads to the same elusive Ru–NHC active species as the preformed [$RuCl_2$(*p*-cymene)(NHC)] family of complexes.

EXPERIMENTAL SECTION

General Information. Unless otherwise specified, all the syntheses were carried out under a dry argon atmosphere using standard Schlenk techniques. Solvents were distilled from appropriate drying agents and deoxygenated prior to use. Imidazol(in)ium-2-thiocarboxylates were prepared according to the literature.[17] The [$RuCl_2$(*p*-cymene)]$_2$ dimer **1** was purchased from Strem. All the other chemicals were obtained from Aldrich. Unless otherwise specified, ^{1}H and ^{13}C NMR spectra were recorded at 298 K with a Bruker DRX 400 spectrometer operating at 400.13 and 100.62 MHz, respectively. Chemical shifts are listed in parts per million downfield from TMS and are referenced from the solvent peaks or TMS. Infrared spectra were recorded with a Perkin–Elmer Spectrum One FT-IR spectrometer. Mass spectral analyses were performed on a Bruker Daltonics SolariX FT-ICR spectrometer operating at 9.4 T in the Laboratory of Mass Spectroscopy of the University of Liège. Elemental analyses were carried out in the Laboratory of Pharmaceutical Chemistry at the University of Liège. Size-exclusion chromatography was performed in THF at 45 °C with a SFD S5200 autosampler liquid chromatograph equipped with a SFD 2000 refractive index detector and a battery of 4 PL gel columns fitted in series (particle size 5 μm; pore sizes 10^5, 10^4, 10^3, and 10^2 Å; flow rate 1 mL/min). The molecular wei ghts (not corrected) are reported versus monodisperse polystyrene or poly(methyl methacrylate) standards used to calibrate the instrument. Gas chromatography was carried out with a Varian 3900 instrument equipped with a flame ionization detector and a WCOT fused silica column (stationary phase CP-Sil 5CB, column length 15 m, inside diameter 0.25 mm, outside diameter 0.39 mm, film thickness 0.25 μm).

Preparation of Ruthenium–Arene Complexes with Thiocarboxylate Ligands. A 50 mL round-bottom flask equipped with a magnetic stirring bar and capped with a three-way stopcock was charged with [$RuCl_2$(*p*-cymene)]$_2$ (**1**; 0.1225 g, 0.2 mmol) and an imidazol(in)ium-2-thiocarboxylate (0.4 mmol). The mixture was cooled in a 3/1 w/w ice/salt bath at −20 °C before dry and cold CH_2Cl_2 (10 mL) was added with a syringe. The resulting orange-red solution was stirred for 1 h at −20 °C. The solvent was then evaporated under high vacuum at −20 °C. The remaining solid was washed with *n*-pentane (3 × 10 mL) and dried under high vacuum.

[$RuCl_2$(p-cymene)(SOC·ICy)] ***(2)***. Orange powder (0.1940 g, 81% yield). ^{1}H NMR (400 MHz, CD_2Cl_2, 263 K): δ 7.20 (s, 2H, Im-$C_{4,5}$), 5.71 (d, $^3J_{HH}$ = 5.9 Hz, 2H, *p*-cym CH_{ar}), 5.49 (d, $^3J_{HH}$ = 5.9 Hz, 2H, *p*-cym CH_{ar}), 4.50 (m, 2H, CHN), 2.83 (sept, $^3J_{HH}$ = 6.9 Hz, 1H, *p*-cym $CH(CH_3)_2$), 2.21 (s, 3H, *p*-cym CH_3), 2.15–2.13 (m, 4H, Cy), 1.86–1.83 (m, 4H, Cy), 1.71–1.68 (m, 2H, Cy), 1.65–1.52 (m, 4H, Cy), 1.46–1.36 (m, 4H, Cy), 1.26 (d, $^3J_{HH}$ = 7.0 Hz, 6H, *p*-cym $CH(CH_3)_2$), 1.23–1.20 (m, 2H, Cy) ppm. ^{13}C NMR (100 MHz, CD_2Cl_2, 263 K): δ 188.2 (COS), 142.9 (Im-C_2), 117.4 (Im-$C_{4,5}$), 101.3 (*p*-cym), 100.6 (*p*-cym), 83.1 (*p*-cym), 80.9 (*p*-cym), 58.7 (CHN), 33.4 (Cy), 31.5 (*p*-cym), 25.3 (Cy), 25.0 (Cy), 22.5 (*p*-cym), 19.0 (*p*-cym) ppm. IR (KBr): $\bar{\nu}$ 3086 (m), 2932 (s), 2857 (s), 1641 (m), 1571 (s), 1482 (s), 1451 (s), 1385 (m), 1271 (w), 1200 (m), 1190 (m), 1171 (m), 1135 (m), 1057 (w), 934 (s), 896 (m), 855 (m), 804 (w) cm^{-1}. HR-MS (ESI+): *m*/*z* calcd for $C_{26}H_{38}ClN_2ORuS$ [(M − Cl)$^+$], 563.143 69; found, 563.146 92. Anal. Calcd for $C_{26}H_{38}Cl_2N_2ORuS$ (598.63): C, 52.17; H, 6.40; N, 4.68; S, 5.36. Found: C, 51.86; H, 6.27; N, 4.97; S, 5.29.

[$RuCl_2$(p-cymene)(SOC·IMes)] ***(3)***. Orange powder (0.2495 g, 93% yield). ^{1}H NMR (400 MHz, CD_2Cl_2, 263 K): δ 7.26 (s, 2H, Im-$C_{4,5}$), 7.08 (s, 4H, *m*-CH), 5.19 (d, $^3J_{HH}$ = 5.9 Hz, 2H, *p*-cym CH_{ar}), 5.13 (d, $^3J_{HH}$ = 5.9 Hz, 2H, *p*-cym CH_{ar}), 2.37 (s, 6H, *p*-CH_3), 2.21 (s, 12H, *o*-CH_3), 1.97 (s, 3H, *p*-cym CH_3), 1.93 (m, $^3J_{HH}$ = 6.9 Hz, 1H, *p*-cym $CH(CH_3)_2$), 0.92 (d, $^3J_{HH}$ = 6.9 Hz, 6H, *p*-cym $CH(CH_3)_2$) ppm. ^{13}C NMR (100 MHz, CD_2Cl_2, 263 K): δ 185.7 (COS), 144.6 (Im-C_2), 141.7 (*p*-C), 135.4 (*o*-C), 131.2 (*ipso*-C), 129.8 (*m*-CH), 122.8 (Im-$C_{4,5}$), 102.1 (*p*-cym), 100.4 (*p*-cym), 83.4 (*p*-cym), 80.8 (*p*-cym), 31.1 (*p*-cym), 22.3 (*p*-cym), 21.4 (*p*-CH_3), 18.6 (*p*-cym), 18.2 (*o*-CH_3) ppm. IR (KBr): $\bar{\nu}$ 3160 (m), 3116 (m), 3091 (m), 2951 (m), 2921 (m), 2863 (m), 1607 (m), 1568 (s), 1488 (s), 1469 (m), 1380 (m), 1229 (m), 1159 (m), 1038 (m), 1006 (m), 910 (s), 855 (m) 806 (w) cm^{-1}. HR-MS (ESI+): *m*/*z* calcd for $C_{32}H_{38}ClN_2ORuS$ [(M − Cl)$^+$], 635.143 69; found, 635.142 43. Anal. Calcd for $C_{32}H_{38}Cl_2N_2ORuS$ (670.70): C, 57.30; H, 5.71; N, 4.18; S, 4.78. Found: C, 56.78; H, 5.61; N, 4.24; S, 4.73.

[$RuCl_2$(p-cymene)(SOC·IDip)] ***(4)***. Orange powder (0.2597 g, 86% yield). ^{1}H NMR (400 MHz, CD_2Cl_2, 263 K): δ 7.59 (t, $^3J_{HH}$ = 7.8 Hz, 2H, *p*-CH), 7.36 (d, $^3J_{HH}$ = 7.8 Hz, 4H, *m*-CH), 7.29 (s, 2H, Im-$C_{4,5}$), 5.25 (d, $^3J_{HH}$ = 5.8 Hz, 2H, *p*-cym CH_{ar}), 5.15 (d, $^3J_{HH}$ = 5.7 Hz, 2H, *p*-cym CH_{ar}), 2.53 (sept, $^3J_{HH}$ = 6.7 Hz, 4H, $CH(CH_3)_2$), 1.91 (s, 3H, *p*-cym CH_3), 1.63 (sept, $^3J_{HH}$ = 6.7 Hz, 1H, *p*-cym $CH(CH_3)_2$), 1.34 (d, $^3J_{HH}$ = 6.7 Hz, 12H, CH_3), 1.15 (d, $^3J_{HH}$ = 6.8 Hz, 12H, CH_3), 0.81 (d, $^3J_{HH}$ = 6.8 Hz, 6H, *p*-cym $CH(CH_3)_2$) ppm. ^{13}C NMR (100 MHz, CD_2Cl_2, 263 K): δ 184.2 (COS), 145.9 (*o*-C), 145.4 (Im-C_2), 131.9 (*p*-CH), 130.8 (*ipso*-C), 125.0 (*m*-CH), 123.5 (Im-$C_{4,5}$), 103.4 (*p*-cym), 99.0 (*p*-cym), 84.0 (*p*-cym), 79.5 (*p*-cym), 30.6 (*p*-cym), 29.6 ($CH(CH_3)_2$), 25.6 (CH_3), 22.9 (CH_3), 22.3 (*p*-cym), 18.6 (*p*-cym) ppm. IR (KBr): $\bar{\nu}$ 3062 (m), 2963 (s), 2929 (m), 2868 (m), 1641 (w), 1572 (s), 1474 (s), 1386 (m), 1365 (m), 1330 (m), 1275 (w), 1210 (m), 1162 (m), 1122 (w), 1060 (m), 1011 (w), 917 (s), 853 (w), 803 (m) cm^{-1}. HR-MS (ESI+): *m*/*z* calcd for $C_{38}H_{50}ClN_2ORuS$ [(M − Cl)$^+$], 719.237 59; found, 719.236 43. Anal. Calcd for $C_{38}H_{50}Cl_2N_2ORuS$ (754.86): C, 60.46; H, 6.68; N, 3.71; S, 4.25. Found: C, 59.69; H, 6.37; N, 3.76; S, 3.86.

[$RuCl_2$(p-cymene)(SOC·SIMes)] ***(5)***. Orange powder (0.2341 g, 87% yield). ^{1}H NMR (400 MHz, CD_2Cl_2, 273 K): δ 7.00 (s, 4H, *m*-CH), 5.11 (d, $^3J_{HH}$ = 5.8 Hz, 2H, *p*-cym CH_{ar}), 5.07 (d, $^3J_{HH}$ = 5.9 Hz, 2H, *p*-cym CH_{ar}), 4.26 (s, 4H, Im-$C_{4,5}$), 2.45 (s, 12H, *o*-CH_3), 2.30 (s, 6H, *p*-CH_3), 1.91 (s, 3H, *p*-cym CH_3), 1.76 (m, $^3J_{HH}$ = 6.6 Hz, 1H, *p*-cym $CH(CH_3)_2$), 0.92 (d, $^3J_{HH}$ = 6.9 Hz, 6H, *p*-cym $CH(CH_3)_2$) ppm. ^{13}C NMR (100 MHz, CD_2Cl_2, 273 K): δ 187.2 (COS), 163.6 (Im-C_2), 141.1 (*p*-C), 136.6 (*o*-C), 130.7 (*ipso*-C), 130.4 (*m*-CH), 101.5 (*p*-cym), 100.7 (*p*-cym), 83.1 (*p*-cym), 81.2 (*p*-cym), 50.8 (Im-$C_{4,5}$), 31.2 (*p*-cym), 22.5 (*p*-cym), 21.4 (*p*-CH_3), 18.6 (*p*-cym), 18.5 (*o*-CH_3) ppm. IR (KBr): $\bar{\nu}$ 2985 (m), 2952 (m), 2921 (m), 2864 (w), 1665 (m), 1609 (m), 1590 (s), 1558 (s), 1515 (m), 1482 (m), 1470 (m), 1390 (m), 1378 (m), 1275 (s), 1213 (w), 1199

dx.doi.org/10.1021/om2006529|*Organometallics* 2011, 30, 6133–6142

(w), 1029 (s), 885 (m), 855 (m), 805 (m) cm^{-1}. HR-MS (ESI+): m/z calcd for $C_{32}H_{40}ClN_2ORuS$ [$(M - Cl)^+$], 637.159 34; found, 637.158 28. Anal. Calcd for $C_{32}H_{40}Cl_2N_2ORuS$ (672.71): C, 57.13; H, 5.99; N, 4.16; S, 4.77. Found: C, 57.14; H, 5.98; N, 4.37; S, 4.53.

*[RuCl$_2$(p-cymene)(SOC·SIDip)] (**6**).* Orange powder (0.2876 g, 95% yield). ^{1}H NMR (400 MHz, CD_2Cl_2, 263 K): δ 7.49 (t, $^3J_{HH}$ = 7.6 Hz, 2H, *p*-CH), 7.30 (d, $^3J_{HH}$ = 7.8 Hz, 4H, *m*-CH), 5.23 (d, $^3J_{HH}$ = 5.7 Hz, 2H, *p*-cym CH_{ar}), 5.12 (d, $^3J_{HH}$ = 5.7 Hz, 2H, *p*-cym CH_{ar}), 4.27 (s, 4H, Im-$C_{4,5}$), 3.14 (sept, $^3J_{HH}$ = 6.7 Hz, 4H, $CH(CH_3)_2$), 1.81 (s, 3H, *p*-cym CH_3), 1.61 (sept, $^3J_{HH}$ = 6.9 Hz, 1H, *p*-cym $CH(CH_3)_2$), 1.41 (d, $^3J_{HH}$ = 6.6 Hz, 12H, CH_3), 1.29 (d, $^3J_{HH}$ = 6.8 Hz, 12H, CH_3), 0.82 (d, $^3J_{HH}$ = 6.8 Hz, 6H, *p*-cym $CH(CH_3)_2$) ppm. ^{13}C NMR (100 MHz, CD_2Cl_2, 263 K): δ 185.6 (COS), 163.0 (Im-C_2), 147 (*o*-C), 131.2 (*ipso*-C), 130.1 (*p*-CH), 125.4 (*m*-CH), 101.9 (*p*-cym), 99.8 (*p*-cym), 83.5 (*p*-cym), 79.5 (*p*-cym), 52.8 (Im-$C_{4,5}$), 30.4 (*p*-cym), 29.5 ($CH(CH_3)_2$), 26.3 (CH_3), 23.6 (CH_3), 22.3 (*p*-cym), 18.5 (*p*-cym) ppm. IR (KBr): $\bar{\nu}$ 3064 (w), 2961 (s), 2928 (m), 2868 (m), 1632 (m), 1593 (s), 1573 (s), 1553 (s), 1465 (m), 1444 (m), 1386 (m), 1365 (w), 1325 (m), 1276 (s), 1181 (m), 1057 (m), 1043 (m), 935 (w), 890 (m), 854 (w), 804 (m) cm^{-1}. HR-MS (ESI+): m/z calcd for $C_{38}H_{52}ClN_2ORuS$ [$(M - Cl)^+$], 721.253 24; found, 721.252 67. Anal. Calcd for $C_{38}H_{52}Cl_2N_2ORuS$ (756.87): C, 60.30; H, 6.92; N, 3.70; S, 4.24. Found: C, 59.76; H, 6.82; N, 4.03; S, 4.25.

X-ray Crystal Structure Determination. Data were collected at 293 K on a Gemini diffractometer (Oxford Diffraction Ltd.) equipped with a Ruby CCD detector using an Enhance (Mo) X-ray source: data collection program, CrysAlis CCD (Oxford Diffraction Ltd.); data reduction, CrysAlis RED (Oxford Diffraction Ltd.); structure solution, SHELXS; structure refinement (on F^2), SHELXL-97;[39] data analysis, PLATON.[40] A multiscan procedure was applied to correct for absorption effects. Hydrogen atom positions were calculated and refined isotropically using a riding model.

*Crystal Data for [RuCl$_2$(p-cymene)(SOC·IMes)] (**3**):* orange-red crystals (obtained by slow diffusion of *n*-pentane into a CH_2Cl_2 solution at −18 °C), a = 12.205(4) Å, b = 16.708(4) Å, c = 17.690(5) Å, β = 119.22(2)°, V = 3148.3(16) Å^3, monoclinic, $P2_1/c$, Z = 4, Mo Kα, μ = 0.761 mm^{-1}, ρ = 1.415 g cm^{-3}, F_{000} = 1384, 10 455 reflections (R_{int} = 0.0731), of which 5100 were unique and 4347 observed ($I > 2\sigma(I)$), R1 (all reflections) = 0.1649, R1 (observed reflections) = 0.0516, wR2 (observed reflections) = 0.0938, S = 0.756, residual density (ΔF) 1.166 and −0.626 e Å^{-3}.

*Crystal Data for [RuCl$_2$(p-cymene)(SOC·SIMes)] (**5**):* orange-red crystals (obtained from CH_2Cl_2 at −18 °C), a = 12.098(2) Å, b = 17.026(4) Å, c = 17.536(5) Å, β = 119.97(2)°, V = 3129.0(8) Å^3, monoclinic, $P2_1/c$, Z = 4, Mo Kα, μ = 0.766 mm^{-1}, ρ = 1.428 g cm^{-3}, F_{000} = 1392, 12 423 reflections (R_{int} = 0.1166), of which 5515 were unique and 3731 observed ($I > 2\sigma(I)$), R1 (all reflections) = 0.1211, R1 (observed reflections) = 0.0786, wR2 (observed reflections) = 0.2117, S = 1.125, residual density (ΔF) 2.271 and −1.956 e Å^{-3}.

ROMP of Cyclooctene. A 25 mL round-bottom flask equipped with a magnetic stirring bar and capped with a three-way stopcock was charged with a ruthenium−arene complex (0.03 mmol). Air was expelled by applying three vacuum−argon cycles before dry chlorobenzene (5 mL) and cyclooctene (1 mL, 7.5 mmol) were added with dried syringes under argon. The reaction mixture was stirred for 2 h in an oil bath at 60 °C. It was irradiated with a 40 W "cold white" fluorescent tube placed 10 cm away from the Pyrex reaction flask. The conversion was monitored by gas chromatography using the cyclooctane impurity of cyclooctene as internal standard. The resulting gel was diluted with chloroform (20 mL) and slowly poured into methanol (300 mL) with vigorous stirring. The precipitated polyoctenamer was filtered with suction, dried overnight under dynamic vacuum, and characterized by size-exclusion chromatography and NMR.

ATRP of MMA. A 25 mL glass tube containing a magnetic stirring bar and capped with a three-way stopcock was charged with a ruthenium−arene complex (0.0117 mmol). Air was expelled by applying three vacuum−nitrogen cycles before methyl methacrylate (1 mL, 9.35 mmol) and ethyl 2-bromo-2-methylpropanoate (0.1 M in toluene, 0.25 mL) were added with dried syringes under nitrogen. The reaction mixture was heated for 16−100 h in an oil bath at 85 °C. It was cooled to room temperature, diluted with THF (5 mL) and poured into *n*-heptane (600 mL) with vigorous stirring. The precipitated polymer was filtered with suction, dried overnight under dynamic vacuum, and characterized by SEC.

Microwave-Assisted Enol Ester Synthesis. A 10 mL glass vial containing a magnetic stirring bar was charged with a ruthenium−arene complex (0.004 mmol), sodium carbonate (0.85 mg, 0.008 mmol), and 4-acetoxybenzoic acid (90 mg, 0.5 mmol). Air was expelled by applying three vacuum−argon cycles before a stock solution containing 1-hexyne (0.75 mmol) and *n*-dodecane (internal standard) in water-saturated toluene (2.6 mL) was added. The vial was capped under nitrogen and heated to 140 °C (monitored by IR sensor) for 10 min in a CEM Discover instrument using a dynamic heating rate program (150 W maximum microwave power). No simultaneous cooling was applied. After rapid air cooling by the unit, the reaction mixture was analyzed by gas chromatography (GC).

Enol Ester Synthesis with Conventional Heating. A 25 mL Schlenk tube equipped with a magnetic stirring bar and capped with a three-way stopcock was charged with a ruthenium−arene complex (0.0092 mmol), sodium carbonate (1.95 mg, 0.0184 mmol), and 4-acetoxybenzoic acid (207 mg, 1.15 mmol). Air was expelled by applying three vacuum−argon cycles before a stock solution containing 1-hexyne (1.725 mmol) and *n*-dodecane (internal standard) in water-saturated toluene (6 mL) was added with a dried syringe under nitrogen. The reaction mixture was stirred in an oil bath at 60 °C until GC analysis of samples withdrawn at regulat time intervals showed that a full conversion had occurred.

■ ASSOCIATED CONTENT

Ⓢ Supporting Information

Figures giving an ORTEP representation of [RuCl$_2$(*p*-cymene)(SOC•IMes)] (**3**) with selected bond lengths and angles and kinetic plots of all the catalytic runs for enol ester synthesis and CIF files giving crystallographic data for complexes **3** and **5**. This material is available free of charge via the Internet at http://pubs.acs.org.

■ AUTHOR INFORMATION

Corresponding Author

*E-mail: l.delaude@ulg.ac.be.

■ ACKNOWLEDGMENTS

The financial support of the "Fonds de la Recherche Scientifique-FNRS", Brussels, Belgium, is gratefully acknowledged for the purchase of major instrumentation. We thank Dr. Nicolas Smargiasso for the HR-MS analyses, Mrs. Bernadette Norberg for the XRD analyses, and Ms. Nelly Tshibalonza Ntumba and Mr. Dario Bicchielli for their help with the catalytic tests.

■ REFERENCES

(1) (a) Arduengo, A. J. III; Harlow, R. L.; Kline, M. *J. Am. Chem. Soc.* **1991**, *113*, 361−363. (b) Arduengo, A. J. III *Acc. Chem. Res.* **1999**, *32*, 913−921.

(2) For monographs, see: (a) *N-Heterocyclic Carbenes in Synthesis*; Nolan, S. P., Ed.; Wiley-VCH: Weinheim, Germany, 2006. (b) *N-Heterocyclic Carbenes in Transition Metal Catalysis*; Glorius, F., Ed.; Springer: Berlin, Germany, 2007; Topics in Organometallic Chemistry Vol. *21*. (c) *N-Heterocyclic Carbenes: From Laboratory Curiosities to Efficient Synthetic Tools*; Díez-González, S., Ed.; Royal Society of Chemistry: Cambridge, U.K., 2010; RSC Catalysis Series Vol. *6*. (d) *N-Heterocyclic Carbenes in Transition Metal Catalysis and Organocatalysis*; Cazin, C. S. J., Ed.; Springer: Dordrecht, The Netherlands, 2011; Catalysis by Metal Complexes Vol. *32*.

(3) Delaude, L. *Eur. J. Inorg. Chem.* **2009**, 1681−1699.
(4) (a) Kuhn, N.; Steimann, M.; Weyers, G. *Z. Naturforsch., B* **1999**, *54*, 427−433. (b) Duong, H. A.; Tekavec, T. N.; Arif, A. M.; Louie, J. *Chem. Commun.* **2004**, 112−113. (c) Van Ausdall, B. R.; Glass, J. L.; Wiggins, K. M.; Aarif, A. M.; Louie, J. *J. Org. Chem.* **2009**, *74*, 7935−7942.
(5) (a) Voutchkova, A. M.; Appelhans, L. N.; Chianese, A. R.; Crabtree, R. H. *J. Am. Chem. Soc.* **2005**, *127*, 17624−17625. (b) Voutchkova, A. M.; Feliz, M.; Clot, E.; Eisenstein, O.; Crabtree, R. H. *J. Am. Chem. Soc.* **2007**, *129*, 12834−12846.
(6) (a) Duong, H. A.; Cross, M. J.; Louie, J. *Org. Lett.* **2004**, *6*, 4679−4681. (b) Bantu, B.; Pawar, G. M.; Decker, U.; Wurst, K.; Schmidt, A. M.; Buchmeiser, M. R. *Chem. Eur. J.* **2009**, *15*, 3103−3109. (c) Naik, P. U.; Petitjean, L.; Refes, K.; Picquet, M.; Plasseraud, L. *Adv. Synth. Catal.* **2009**, *351*, 1753−1756. (d) Riduan, S. N.; Zhang, Y.; Ying, J. Y. *Angew. Chem., Int. Ed.* **2009**, *48*, 3322−3325. (e) Kayaki, Y.; Yamamoto, M.; Ikariya, T. *Angew. Chem., Int. Ed.* **2009**, *48*, 4194−4197.
(7) Tudose, A.; Delaude, L.; André, B.; Demonceau, A. *Tetrahedron Lett.* **2006**, *47*, 8529−8533.
(8) Tudose, A.; Demonceau, A.; Delaude, L. *J. Organomet. Chem.* **2006**, *691*, 5356−5365.
(9) Grotevendt, A.; Bartolome, M.; Nielsen, D. J.; Spannenberg, A.; Jackstell, R.; Cavell, K. J.; Oro, L. A.; Beller, M. *Tetrahedron Lett.* **2007**, *48*, 9203−9207.
(10) Delaude, L.; Sauvage, X.; Demonceau, A.; Wouters, J. *Organometallics* **2009**, *28*, 4056−4064.
(11) Sauvage, X.; Demonceau, A.; Delaude, L. *Adv. Synth. Catal.* **2009**, *351*, 2031−2038.
(12) Sauvage, X.; Zaragoza, G.; Demonceau, A.; Delaude, L. *Adv. Synth. Catal.* **2010**, *352*, 1934−1948.
(13) (a) Sheldrick, W. S.; Schönberg, A.; Singer, E.; Eckert, P. *Chem. Ber* **1980**, *113*, 3605−3609. (b) Krasuski, W.; Nikolaus, D.; Regitz, M. *Liebigs Ann. Chem.* **1982**, 1451−1465. (c) Kuhn, N.; Bohnen, H.; Henkel, G. *Z. Naturforsch., B* **1994**, *49*, 1473−1480. (d) Kuhn, N.; Niquet, E.; Steimann, M.; Walker, I. *Z. Naturforsch., B* **1999**, *54*, 1181−1187. (e) Delaude, L.; Demonceau, A.; Wouters, J. *Eur. J. Inorg. Chem.* **2009**, 1882−1891.
(14) (a) Naeem, S.; Thompson, A. L.; Delaude, L.; Wilton-Ely, J. D. E. T. *Chem. Eur. J.* **2010**, *16*, 10971−10974. (b) Naeem, S.; Thompson, A. L.; White, A. J. P.; Delaude, L.; Wilton-Ely, J. D. E. T. *Dalton Trans.* **2011**, *40*, 3737−3747.
(15) Naeem, S.; Delaude, L.; White, A. J. P.; Wilton-Ely, J. D. E. T. *Inorg. Chem.* **2010**, *49*, 1784−1793.
(16) Willem, Q.; Nicks, F.; Sauvage, X.; Delaude, L.; Demonceau, A. *J. Organomet. Chem.* **2009**, *694*, 4049−4055.
(17) Hans, M.; Wouters, J.; Demonceau, A.; Delaude, L. *Eur. J. Org. Chem.* **2011**, (doi: 10.1002/ejoc.201101286).
(18) Chia, E. Y.; Naeem, S.; Delaude, L.; White, A. J. P.; Wilton-Ely, J. D. E. T. *Dalton Trans.* **2011**, *40*, 6645−6658.
(19) See for example: (a) Bennett, M. A.; Smith, A. K. *J. Chem. Soc., Dalton Trans.* **1974**, 233−241. (b) Jan, D.; Delaude, L.; Simal, F.; Demonceau, A.; Noels, A. F. *J. Organomet. Chem.* **2000**, *606*, 55−64. (c) Solari, E.; Gauthier, S.; Scopelliti, R.; Severin, K. *Organometallics* **2009**, *28*, 4519−4526. (d) Borguet, Y.; Sauvage, X.; Zaragoza, G.; Demonceau, A.; Delaude, L. *Organometallics* **2010**, *29*, 6675−6686.
(20) Özdemir, I.; Yaşar, S.; Demir, S.; Çetinkaya, B. *Heteroat. Chem.* **2005**, *16*, 557−561.
(21) Savant, V. V.; Gopalakrishnan, J.; Patel, C. C. *Inorg. Chem.* **1970**, *9*, 748−751.
(22) (a) Gould, R. O.; Stephenson, T. A.; Thomson, M. A. *J. Chem. Soc., Dalton Trans.* **1978**, 769−775. (b) El-Hinnawi, M. A.; Sumadi, M. L.; Esmadi, F. T.; Jibril, I.; Imhof, W.; Huttner, G. *J. Organomet. Chem.* **1989**, *377*, 373−381. (c) Jibril, I.; Esmadi, F. T.; Al-Masri, H.; Zsolnai, L.; Huttner, G. *J. Organomet. Chem.* **1996**, *510*, 109−116. (d) El-khateeb, M.; Jazzazi, T. M. A.; Görls, H.; Al-Shboul, T. M. A.; Westerhausen, M. *Transition Met. Chem.* **2011**, *36*, 29−33.
(23) Nakayama, J.; Kitahara, T.; Sugihara, Y.; Sakamoto, A.; Ishii, A. *J. Am. Chem. Soc.* **2000**, *122*, 9120−9126.
(24) (a) Le Bozec, H.; Touchard, D.; Dixneuf, P. H. *Adv. Organomet. Chem.* **1989**, *29*, 163−247. (b) Bennett, M. A. *Coord. Chem. Rev.* **1997**, *166*, 225−254. Therrien, B. *Coord. Chem. Rev.* **2009**, *253*, 493−519.
(25) Allen, F. H.; Kennard, O.; Watson, D. G.; Brammer, L.; Orpen, A. G.; Taylor, R. *J. Chem. Soc. Perkin Trans 2* **1987**, S1−S19.
(26) (a) Martin, N. H.; Allen, N. W. III; Moore, K. D.; Vo, L. *J. Mol. Struct. (THEOCHEM)* **1998**, *454*, 161−166. (b) Martin, N. H.; Allen, N. W. III; Moore, J. C. *J. Mol. Graph. Model.* **2000**, *18*, 242−246−300−301.
(27) (a) Slugovc, C.; Perner, B.; Stelzer, F.; Mereiter, K. *Organometallics* **2004**, *23*, 3622−3626. (b) Ben-Asuly, A.; Tzur, E.; Diesendruck, C. E.; Sigalov, M.; Goldberg, I.; Lemcoff, N. G. *Organometallics* **2008**, *27*, 811−813.
(28) Lo, C.; Cariou, R.; Fischmeister, C.; Dixneuf, P. H. *Adv. Synth. Catal.* **2007**, *349*, 546−550.
(29) (a) Sauvage, X.; Borguet, Y.; Noels, A. F.; Delaude, L.; Demonceau, A. *Adv. Synth. Catal.* **2007**, *349*, 255−265. (b) Maj, A.; Delaude, L.; Demonceau, A.; Noels, A. F. *J. Organomet. Chem.* **2007**, *692*, 3048−3056. (c) Sauvage, X.; Borguet, Y.; Zaragoza, G.; Demonceau, A.; Delaude, L. *Adv. Synth. Catal.* **2009**, *351*, 441−455. (d) Borguet, Y.; Sauvage, X.; Zaragoza, G.; Demonceau, A.; Delaude, L. *Organometallics* **2011**, *20*, 2730−2738.
(30) (a) Delaude, L.; Demonceau, A.; Noels, A. F. *Chem. Commun* **2001**, 986−987. (b) Delaude, L.; Szypa, M.; Demonceau, A.; Noels, A. F. *Adv. Synth. Catal.* **2002**, *344*, 749−756.
(31) Ahr, M.; Thieuleux, C.; Copéret, C.; Fenet, B.; Basset, J.-M. *Adv. Synth. Catal.* **2007**, *349*, 1587−1591.
(32) For a recent review on light-induced olefin metathesis, see: Vidavsky, Y.; Lemcoff, N. G. *Beilstein J. Org. Chem.* **2010**, *6*, 1099−1105.
(33) Delaude, L.; Demonceau, A.; Noels, A. F. *Curr. Org. Chem.* **2006**, *10*, 203−215.
(34) Delaude, L.; Delfosse, S.; Richel, A.; Demonceau, A.; Noels, A. F. *Chem. Commun* **2003**, 1526−1527.
(35) For selected reviews, see: (a) Bruneau, C.; Dixneuf, P. H. *Chem. Commun* **1997**, 507−512. (b) Alonso, F.; Beletskaya, I. P.; Yus, M. *Chem. Rev.* **2004**, *104*, 3079−3160. (c) Dragutan, V.; Dragutan, I.; Delaude, L.; Demonceau, A. *Coord. Chem. Rev.* **2007**, *251*, 765−794.
(36) For a discussion of the catalytic importance of H_2O and Na_2CO_3, see: Nicks, F.; Aznar, R.; Sainz, D.; Muller, G.; Demonceau, A. *Eur. J. Org. Chem.* **2009**, 5020−5027.
(37) Nicks, F.; Libert, L.; Delaude, L.; Demonceau, A. *Aust. J. Chem.* **2009**, *62*, 227−231.
(38) Ledoux, N.; Allaert, B.; Verpoort, F. *Eur. J. Org. Chem.* **2007**, 5578−5583.
(39) Sheldrick, G. M. *SHELXL-97, Program for the Refinement of Crystal Structures*; University of Göttingen, Göttingen, Germany, 1997.
(40) Spek, A. L. *PLATON, A Multipurpose Crystallographic Tool*; Utrecht University: Utrecht, The Netherlands, 2005.